Cell Host & Microbe
Article

Actin and Intermediate Filaments Stabilize the *Chlamydia trachomatis* Vacuole by Forming Dynamic Structural Scaffolds

Yadunanda Kumar[1] and Raphael H. Valdivia[1,*]
[1]Department of Molecular Genetics and Microbiology and Center for Microbial Pathogenesis, Duke University Medical Center, Durham, NC 27710, USA
*Correspondence: valdi001@mc.duke.edu
DOI 10.1016/j.chom.2008.05.018

SUMMARY

The obligate intracellular bacterial pathogen *Chlamydia trachomatis* replicates within a large vacuole or ''inclusion'' that expands as bacteria multiply but is maintained as an intact organelle. Here, we report that the inclusion is encased in a scaffold of host cytoskeletal structures made up of a network of F-actin and intermediate filaments (IF) that act cooperatively to stabilize the pathogen-containing vacuole. Formation of F-actin at the inclusion was dependent on RhoA, and its disruption led to the disassembly of IFs, loss of inclusion integrity, and leakage of inclusion contents into the host cytoplasm. In addition, IF proteins were processed by the secreted chlamydial protease CPAF to form filamentous structures at the inclusion surface with altered structural properties. We propose that *Chlamydia* has co-opted the function of F-actin and IFs to stabilize the inclusion with a dynamic, structural scaffold while minimizing the exposure of inclusion contents to cytoplasmic innate immune-surveillance pathways.

INTRODUCTION

Chlamydiae sps are obligate intracellular bacterial pathogens of humans and animals. In humans, *Chlamydia trachomatis* infects ocular and genital epithelial surfaces to cause diseases such as conjunctivitis, salpingitis, and urethritis, and chronic inflammation from recurrent chlamydial infections can lead to devastating sequela such as blinding trachoma, pelvic inflammatory disease, and infertility (Schachter, 1999).

C. trachomatis displays a biphasic life cycle, with an infectious, metabolically inactive elementary body (EB) form, and a noninfectious, replicative reticulate body (RB) form (Belland et al., 2004). Shortly after invasion, EBs differentiate into RBs and replicate within a membrane-bound parasitophorous vacuole termed an ''inclusion.'' The inclusion expands as bacteria replicate and is maintained as a large intact organelle. It has been proposed that attachment to the inclusion membrane maintains RBs in a replicative state, while detachment triggers the developmental transition to EBs (Peters et al., 2007). Therefore, the morphology of the inclusion may influence chlamydial replication with small number of large inclusions within a cell leading to the highest yield of EBs (Wilson et al., 2006). The expansion of inclusions is likely fueled by the acquisition of membrane lipids from Golgi-derived vesicles (Carabeo et al., 2003) and multivesicular bodies (MVBs) (Beatty, 2006). Because vesicular transport and the morphology of membrane compartments is linked to the function of the cytoskeleton (Musch, 2004; Rodriguez-Boulan et al., 2005; Toivola et al., 2005), it is likely that the mature inclusion interacts extensively with cytoskeletal elements.

The major components of the mammalian cytoskeleton, microtubules, actin microfilaments, and intermediate filaments (IFs) differ widely in their structural and biochemical properties. Actin microfilaments are 10 nm thick homopolymers (Wear et al., 2000), while microtubules are 25 nm thick hetero-oligomers of α and β tubulin that assemble unidirectionally (Desai and Mitchison, 1997). Both actin filaments and microtubules perform functions ranging from providing structural stability to regulating intracellular vesicle trafficking, cell migration, and division (Rodriguez-Boulan et al., 2005). In contrast, IFs are formed by a diverse family of proteins (>70) that share a tripartite domain structure consisting of an N-terminal head domain, middle coiled coil containing Rod-domain, and a C-terminal tail (Herrmann et al., 2007). IF assembly is largely energy independent and involves lateral association of dimers and tetramers into 60 nm long unit-length filaments that subsequently anneal longitudinally to give rise to mature filaments. IFs assemble either as obligate heteropolymers (Type I and Type II keratins and neurofilaments) or homopolymers (Type III vimentin and desmin-like IFs) and exist as separate filament systems within the same cell (Herrmann et al., 2007). Although IFs are traditionally viewed as scaffolds that provide mechanical support, recent studies suggest that IFs can also regulate cell signaling, protein synthesis, and vesicular trafficking (Kim and Coulombe, 2007). These three cytoskeletal elements exist as dynamic structures by interacting with each other directly and through a variety of bridging molecules (Fuchs and Karakesisoglou, 2001). Therefore, disruption of one cytoskeletal structure can impact the organization and function of the others.

Like many intracellular pathogens, *Chlamydiae* target the host cytoskeleton to facilitate their entry into the mammalian host (Rottner et al., 2005). For *C. trachomatis*, activation of the small GTPase Rac1 and recruitment of WAVE2, an activator of the Arp2/3 actin nucleator complex, induce localized actin polymerization at attachment sites to promote bacterial entry (Carabeo et al., 2002). This process is aided by the chlamydial protein

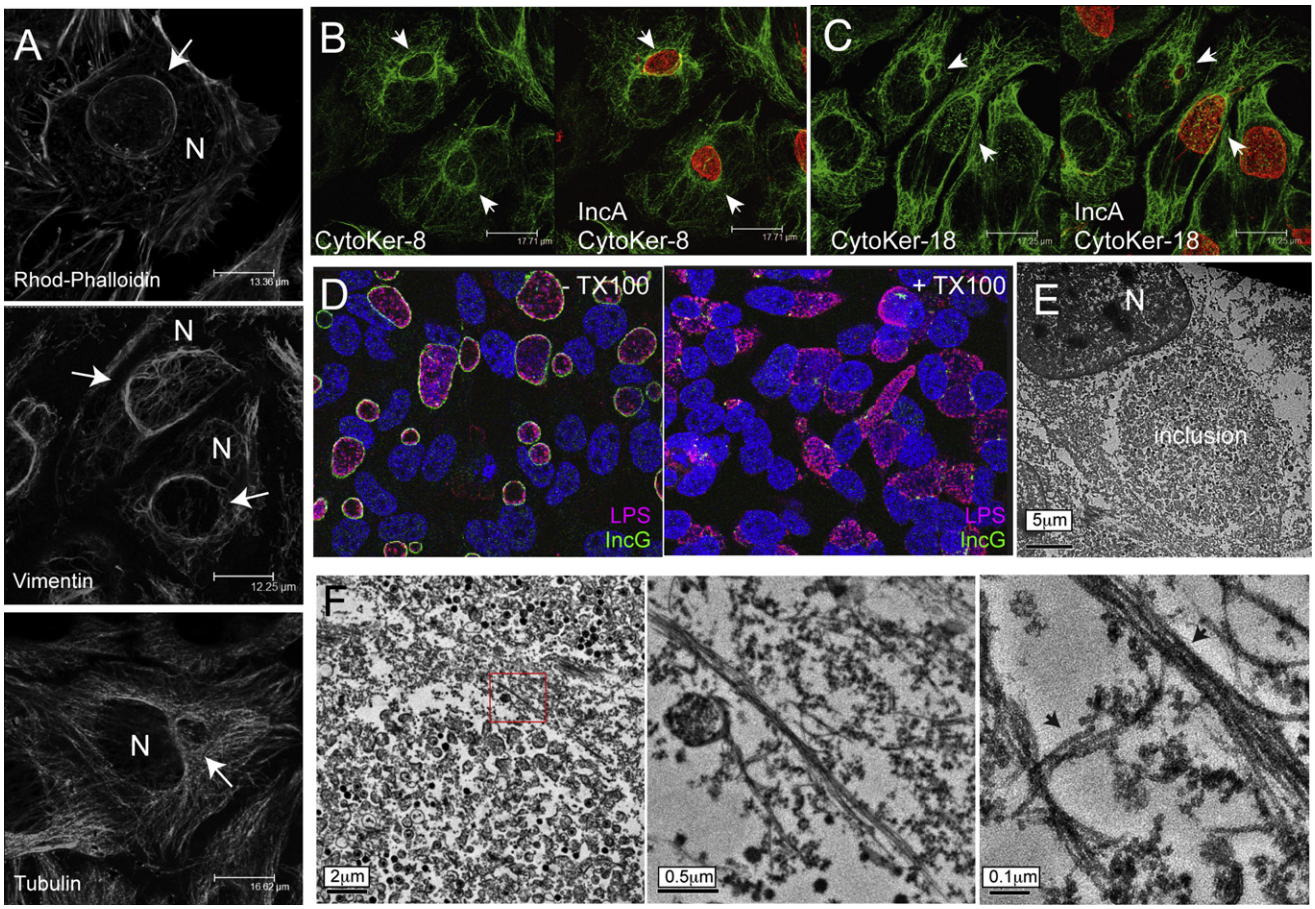

Figure 1. Actin and Intermediate Filaments Are Reorganized at the Periphery of the *C. trachomatis* Inclusion

(A) Architecture of the host cytoskeleton in *Chlamydia*-infected cells. HeLa cells were infected with *C. trachomatis* LGV-L2 for 26–30 hr, fixed, and processed for immunofluorescence microscopy. F-actin was detected with rhodamine-phalloidin, and IFs and microtubules were detected with antibodies to vimentin and α-tubulin, respectively. Note the assembly of actin and vimentin filaments at the inclusion (arrows).

(B and C) Cages of cytokeratin-8 and keratin-18 filaments assemble at the inclusion. HeLa cells were infected as in (A), fixed, and cytokeratins detected with antibodies to cytokeratin-8 (B) and keratin-18 (C). Inclusions (arrows) were detected with anti-IncA antibodies (red).

(D and E) The lumenal contents of inclusions are resistant to detergent extraction. HeLa cells were infected for 30 hr and either left untreated (left) or treated (right) with 1% Triton X-100 (Tx-100) for 5 min at 4°C. Cells were fixed and stained with anti-chlamydial LPS (red), IncG (green) antibodies, and the DNA stain TO-PRO-3 (blue). Transmission electron micrographs of detergent-extracted cells show the intact morphology of inclusion and the loss of membranes at the periphery of the inclusion (E).

(F) Parallel filaments localize to the inclusion periphery. Transmission electron micrographs reveal F-actin (~10nm) filament bundles (arrows) associated with the periphery of the inclusion.

Tarp, a nucleator of actin polymerization, which is translocated into the host cell during invasion (Clifton et al., 2004). The nascent inclusion also interacts with the microtubule network to promote its migration to the microtubule organizing center (Grieshaber et al., 2003). The role of the host cytoskeleton during the replicative phase of the chlamydial life cycle is less well characterized, although recent findings implicate actin filaments in the process of bacterial exit from the infected cell (Hybiske and Stephens, 2007).

Because membrane traffic and the shape of subcellular structures are intimately linked to the function of the cytoskeleton, we hypothesized that the inclusion interacts extensively with cytoskeletal elements. In this study, we report that *Chlamydia* co-opts RhoA function to assemble a stable structural scaffold around the inclusion consisting of F-actin and IFs. The consequence of loss of inclusion integrity is the spillage of bacterial contents to the host cytoplasm, leading to the activation of innate immune responses.

RESULTS

Actin and IFs Assemble on the *Chlamydia* Inclusion

To assess how the host cytoskeleton interacts with mid-to-late cycle inclusions (24–30 hr), we surveyed the subcellular localization of F-actin, IFs, and microtubules by staining with rhodamine-labeled phalloidin or by indirect immunofluorescence with anti-α-tubulin and vimentin antibodies. Although the morphology of stress fibers and cortical actin was not affected in infected cells, we observed the formation of a compact, uniform ring of F-actin around the inclusion (Figure 1A). Similarly, we found a dramatic reorganization of vimentin to the inclusion with loss of vimentin at the cell periphery (Figure 1A). In contrast, the microtubule

network did not appear overtly perturbed. However, because the physical displacement of microtubules by the inclusion, especially in later stages of infection, can obscure the visualization of specific interactions, we cannot discount the possibility that the inclusion may also interact with microtubules. Three-dimensional reconstruction of serial laser-scanning confocal sections confirmed that the inclusion was surrounded by a meshwork of actin and vimentin filaments (see Movie S1 available online). The recruitment of these structures is unlikely to be an artifact of the fixation or staining methodology, since cells expressing a GFP-tagged F-actin binding domain of moesin or GFP-tagged vimentin recruited the reporter fusion proteins to the inclusion (see Figure S1 available online). Furthermore, the reorganization of IF proteins was not restricted to vimentin since the two main cytokeratins expressed in HeLa cells, keratin-8 and keratin-18, also encased inclusions (Figures 1B and 1C). Association of F-actin and IFs with the inclusion surface increased progressively from ~20 hr postinfection until the end of the life cycle (Figure S2). These findings indicate that establishment of a mature inclusion is accompanied by a significant rearrangement of cytoskeletal elements during the mid-to-late stages of the infectious cycle, when maximal inclusion expansion occurs. F-actin recruitment and IF rearrangement at the inclusion were also apparent in cells infected with several *Chlamydia* and *Chlamydophila* species, suggesting that cytoskeletal rearrangements are a conserved feature of *Chlamydiae* infections (Figure S3).

Because IFs are stable structures that provide mechanical support to cells, we hypothesized that the recruitment of these cytoskeletal components to the inclusion would impart structural stability to this organelle. A hallmark property of stable cytoskeletal structures is their resistance to detergent extraction: nonionic detergents solubilize all membranes in live cells while leaving the cytoskeletal network and the host nuclear matrix intact (Vale et al., 1985). We treated *Chlamydia*-infected cells with 1% Triton X-100 (Tx-100) and assessed inclusion morphology. Remarkably, the overall organization of the inclusion was unaffected with bacterial contents sequestered within the inclusion lumen despite the complete solubilization of the inclusion membrane (Figure 1D). These results suggest that the morphology of the inclusion, like the nuclear matrix, is maintained by a stable arrangement of actin and IFs. We analyzed detergent-extracted cells by transmission electron microscopy and confirmed that inclusion contents remained sequestered (Figure 1E). Closer inspection of the inclusion-cytoplasm interface revealed the presence of parallel filamentous bundles (Figure 1F). The majority of the fiber components of these bundles had a mean diameter of 10.2 nm (± 0.5 nm, n = 20), which is consistent with reported thickness of F-actin fibers under the staining conditions used (Maupin and Pollard, 1983).

F-actin Is Essential for Maintenance of Inclusion Morphology and Integrity

The unusual stable properties of inclusions prompted us to assess the role of actin and intermediate filaments in maintaining inclusion morphology and integrity. We determined that F-actin rings at the inclusion were lost within 15 min of treatment with various F-actin polymerization inhibitors—cytochalasin-D (Cyto-D), latrunculin-A, and latrunculin-B (Lat-A and Lat-B) (Fenteany and Zhu, 2003) (Figure 2A)—and that F-actin rings were reformed within 3 hr of Lat-B removal (Figure 2B). Next, we tested the effect of these inhibitors on inclusion membrane morphology and stability. Disruption of F-actin resulted in dramatic remodeling of the inclusion membrane (Figure 2C), including a 5–10-fold increase in the formation of IncA-positive fibers (Figure S4A). IncA-fibers have been previously shown to accumulate during antibiotic treatment (Brown et al., 2002), but their function is unknown.

Concomitant with these changes, LPS staining (Figure 2C) was observed in the host cytoplasm, suggesting a loss of inclusion membrane integrity. To confirm this, we monitored the subcellular localization of bacteria in latrunculin-treated cells by a variety of methods. First, we gently permeabilized the plasma membrane of infected cells and labeled inclusion membranes and bacteria with anti-IncA and anti-Omp2 antibodies, respectively. Omp2-positive bacteria were seen scattered in the cytoplasm outside the confines of IncA-positive inclusion membranes (Figures 2D and 2E). Upon removal of Lat-B, inclusions regained their original shape, but Omp-2-positive bacteria remained in the cytoplasm (Figures 2D–2F). These findings were consistent with our analysis of LatA-treated infected cells by electron microscopy, where we observed bacteria in the cytoplasm and zones of inclusion membrane disruption where cytoplasmic and inclusion lumen contents appeared to mix (Figure 2G). This is likely the result of decreased stability of large inclusions and their fragmentation during F-actin disassembly. Time-lapse images of live infected cells where the inclusion membrane was labeled with Lda3-EGFP (Cocchiaro et al., 2008) revealed a rapid fragmentation of inclusion upon LatA treatment (Figure 2H and Movie S2). We predicted that bacteria in the cytoplasm would be engaged by cytoplasmic microbial pattern recognition receptors leading to the activation of a cytokine response. Consistent with this, IL-8 mRNA levels increased significantly in Lat-B-treated infected cells (Figure 2I), and this activation was blocked by ERK inhibitors (Buchholz and Stephens, 2007).

Finally, we tested if disruption of F-actin correlated with a loss of the inclusion's stable cytoskeletal properties. Short treatments with Lat-A and CytoD significantly decreased the inclusion's resistance to extraction with 1% Tx-100 (Figures 2J and 2K). In contrast, disruption of microtubules with nocodazole did not lead to obvious changes in inclusion morphology, fiber formation, or inclusion stability (Figures 2A, 2J, and S4A). These results indicate that maintenance of inclusion shape and integrity requires intact actin microfilaments.

RhoA Is Required for the Assembly of F-Actin Rings at the Inclusion

Because the uniform ring-like morphology of actin filaments around the inclusion was reminiscent of transverse actin stress fibers, we tested their contribution to the inclusion's cytoskeletal properties. Actin stress fibers are bundles of actin and myosin filaments that are stabilized by α-actinin (Hotulainen and Lappalainen, 2006) and regulated by Rho-associated protein kinase (ROCK) (Katoh et al., 2007). In addition, the RhoA, B, and C family of small GTPases regulate the assembly and stability of stress fibers by activating formins (Jaffe and Hall, 2005) and ROCK (Wheeler and Ridley, 2004). Consequently, inhibitors of ROCK (Y-27632) (Narumiya et al., 2000), myosin-II (Blebbistatin)

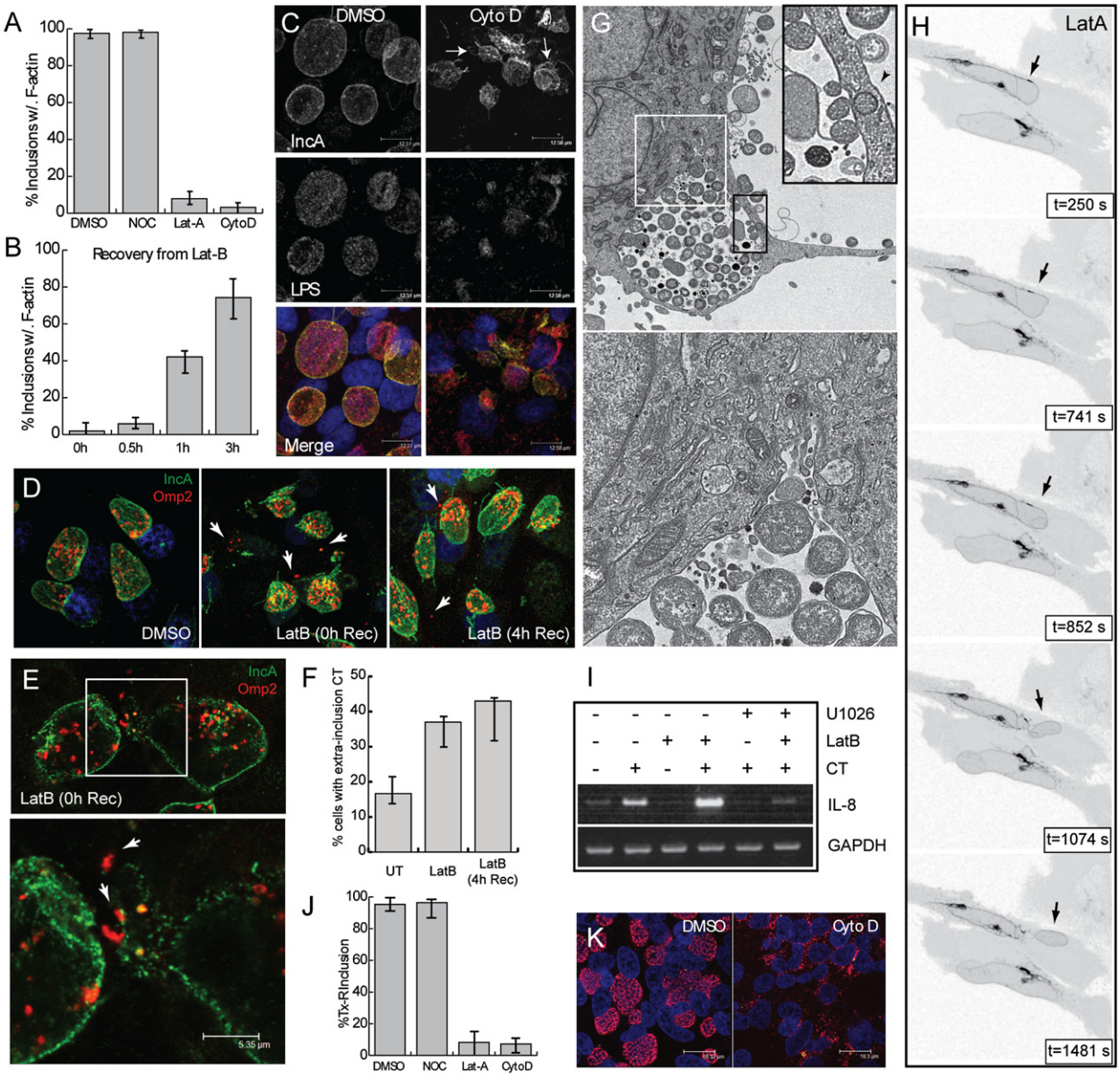

Figure 2. F-Actin Assembly Is Required for Inclusion Integrity and Stability

(A and B) F-actin recruitment to the inclusion is dynamic. HeLa cells were infected with LGV-L2 for 30 hr, and the number of F-actin positive inclusions was quantified after treatment with latrunculin-A (Lat-A 400 nM, 15 min), nocodazole (Noc, 10 μM, 2 hr), and cytochalasin D (Cyto D, 1 μM, 30 min) (A) or after recovery from a 30 min treatment with latrunculin B (Lat-B, 0.5 μM) (B) (n = 150).

(C) Disruption of F-actin leads to alterations in inclusion-membrane morphology. HeLa cells infected with LGV-L2 for 30 hr were treated with DMSO or Cyto D (1 μM, 30 min) and immunostained with anti-IncA and chlamydial LPS antibodies to detect inclusion membranes and bacteria, respectively. Note the accumulation of deformed inclusions (arrows).

(D–G) Disruption of F-actin leads to the release of inclusion contents into the cytoplasm. Infected HeLa cells were treated with DMSO or Lat-B, followed by washout of the drug for 4 hr. Cells were permeabilized with digitonin and IncA, and Omp2 was detected by immunofluorescence microscopy. Note the presence of Omp2-positive bacteria (arrows) not associated with IncA (D and E). Electron micrographs of LatA-treated cells (G) indicate potential rupture sites at the inclusion membrane (white box, bottom panel) and bacteria (arrow) in the cytoplasm (black box, upper right).

(H) Fragmentation of inclusions in response to LatA treatment. Time-lapse series of infected cells where inclusion membranes are labeled with Lda3-EGFP. Note formation of satellite inclusions (arrows) after Lat treatment.

(I) F-actin disruption leads to increased IL-8 activation in infected cells. IL-8 expression levels were assessed by RT-PCR of total RNA isolated from infected and uninfected HeLa cells after Lat-B treatment, as in (D). The ERK inhibitor U1026 was added as a control for *Chlamydia*-mediated IL-8 activation.

(J and K) Disruption of F-actin renders the inclusion sensitive to detergent extraction. Infected HeLa (30 hr) were treated as in (A). The percentage of Tx-100-resistant inclusions (Figure 1D), as assessed by staining with anti-chlamydial LPS (G), was quantified (n = 200). The error bars represent positive and negative deviations from the mean of three independent experiments.

(Straight et al., 2003), or RhoA–C (clostridial C3-transferase) (Aktories and Just, 2005) lead to the disassembly of stress fibers. In *Chlamydia*-infected cells, treatment with Blebbistatin and Y-27632 resulted in a complete loss of stress fibers from the host cytoplasm (not shown) but did not alter the formation of F-actin rings at the inclusion or its sensitivity to detergent extraction (Figures 3A and 3B). In contrast, C3-transferase disrupted the F-actin ring formation and led to their increased sensitivity to detergent extraction (Figures 3A, 3B, and S5A). We tested the contribution of RhoA to this process, by inhibiting its expression in HeLa cells with small interfering RNA duplexes (siRNAs) (Figure S5). We found that depletion of RhoA significantly reduced the proportion of inclusions with intact F-actin rings (Figure 3C). In addition, we determined that siRNA-mediated depletion of Rac1 and Cdc42 did not affect the formation of F-actin rings, suggesting that the role of RhoA in inclusion-associated F-actin is direct. We tested if RhoA was recruited to the inclusion by monitoring the localization of EGFP-tagged constitutively active (Q63L), inactive (T19N), and wild-type forms of RhoA. All three RhoA forms associated with the periphery of the inclusion with RhoA (Q63L), showing a distinct ring-like pattern at the inclusion membrane (Figures 3D, 3E, and data not shown), indicating that the assembly of F-actin rings is RhoA dependent and that RhoA is recruited to the inclusion independently of its nucleotide-bound status.

Vimentin and Actin Filaments Act Cooperatively to Stabilize to the Inclusion

Next, we determined the role of vimentin on inclusion morphology and stability by infecting mouse embryonic fibroblasts (MEFs) derived from vimentin-knockout mice (Colucci-Guyon et al., 1994). Since MEFs do not express cytokeratins (Colucci-Guyon et al., 1994), we were able to assess vimentin's contribution to the cytoskeletal properties of the inclusion without confounding effects from other IF proteins. Unlike $Vim^{+/+}$ MEFs, inclusions in $Vim^{-/-}$ MEFs were readily disrupted by treatment with Tx-100 (Figures 4A and 4B). Inclusions in infected $Vim^{-/-}$ MEFs had F-actin rings indicating that actin recruitment to the inclusion is not dependent on IFs. However, these F-actin rings appeared disordered and lacked the compact morphology of rings formed in wild-type MEFs (Figure 4C). Consistent with our finding that the accumulation of inclusion-membrane fibers correlates with decreased levels of inclusion stability, we observed enhanced levels of IncA-positive fibers in $Vim^{-/-}$ MEFs (Figures S4C and S4D).

Because the IF architecture is modulated by actin and microtubules (Herrmann et al., 2007), we tested if the recruitment of vimentin to the inclusion was dependent on these structures. Disruption of microtubules resulted in a collapse of the vimentin network to the periphery of the nuclear envelope (not shown) but did not affect the vimentin envelope surrounding the inclusion (Figure 4D). In contrast, inhibitors of F-actin completely displaced vimentin filaments from the inclusion into aggregates of parallel filaments (Figures 4D and 4E). Similarly, treatment with C3-transferase also displaced vimentin from the inclusions, indicating that IF association with inclusions is specific to a Rho-dependent function (Figure 4D). Finally, this process is reversible since removal of Lat-B led to the reassembly of vimentin cages in >70% of the inclusions within 3hr (Figures 4E and 4F).

These results indicate that the recruitment of vimentin filaments to the inclusion is dynamic, reversible, and requires RhoA-dependent F-actin assembly. Furthermore, actin and vimentin filaments independently contribute to maintaining the integrity of the inclusion.

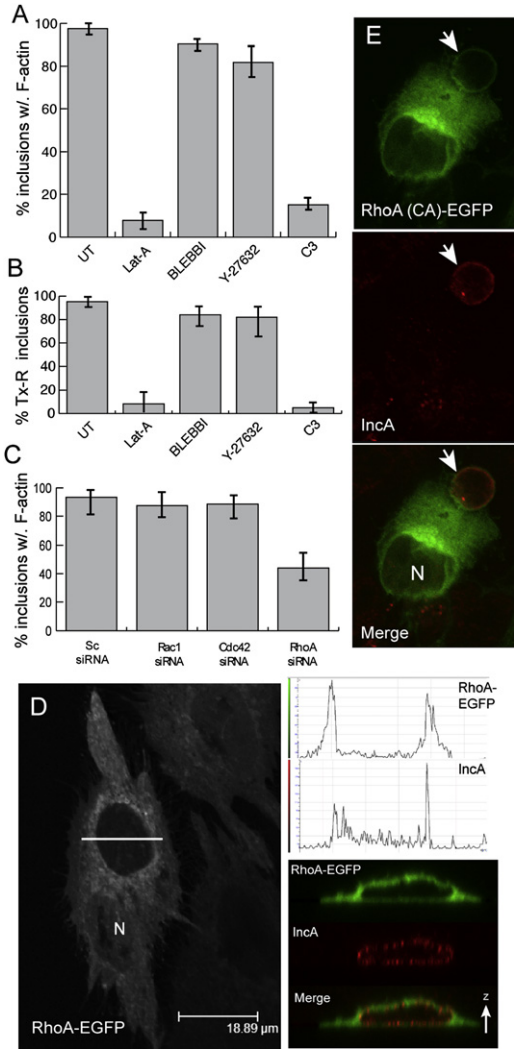

Figure 3. F-Actin Recruitment to the Inclusion Requires RhoA Function

(A–C) RhoA is required for F-actin assembly and inclusion stability. HeLa cells were infected with LGV-L2 for 30 hr and treated with Lat-A, Blebbistatin (50 μM, 1hr), the ROCK inhibitor Y-27632 (20 μM, 1 hr), or C3-transferase (3 μg/ml, 6 hr). Cells were fixed and stained for F-actin and IncA or extracted with 1% Tx-100 prior to fixation, followed by immunostaining with anti-LPS antibodies. The percentage of inclusions with intact F-actin rings (A) or that were resistant to detergent extraction (B) was determined as in Figure 2. UT means untreated. In (C), the expression of Rho proteins was inhibited by transfection of specific siRNAs, and the percentage of inclusions with F-actin-ring was determined as in Figure 2 (n = 150). A scrambled (Sc) siRNA (QIAGEN) was used as a nonspecific control.

(D and E) RhoA is recruited to the periphery of the inclusion. HeLa cells were infected with RhoA-EGFP (D) or a constitutively active RhoA variant Q67L (E). Note the accumulation of the tagged proteins at the periphery of the IncA-positive inclusion membranes. Corresponding zy confocal scans and quantification of EGFP and IncA signal intensity at a representative crosssection of the inclusion is shown (D, right panels).

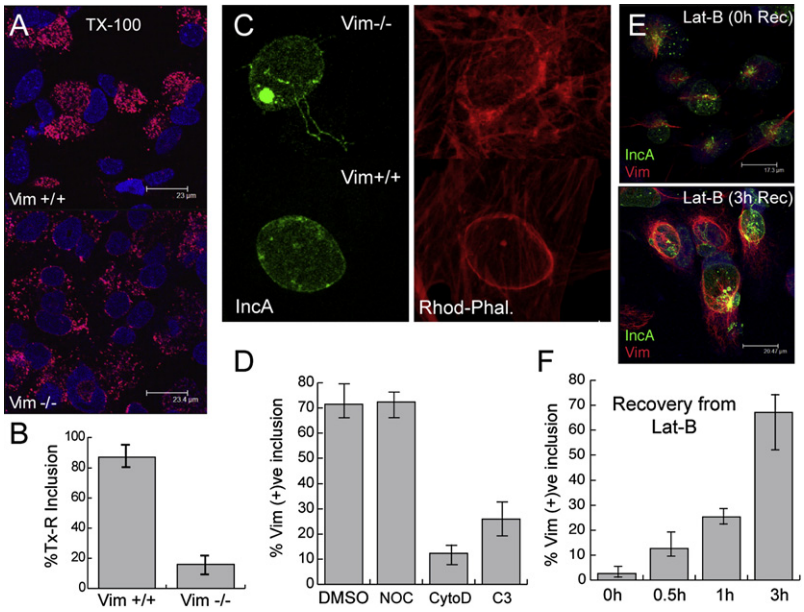

Figure 4. Vimentin Filaments Contribute to Inclusion Stability

(A and B) Inclusions in vimentin-deficient fibroblasts are sensitive to detergent extraction. MEFs derived from vimentin-knockout mice (MTF16-Vim$^{-/-}$) or wild-type littermate controls (MTF6-Vim$^{+/+}$) were infected with LGV-L2 for 30 hr, treated live with 1% Tx-100, processed for immunofluorescence as in Figure 1D (A), and the frequency of detergent-resistant inclusions was assessed (B).

(C) Morphology of actin rings in vimentin deficient MEFs. Vim$^{-/-}$ and Vim$^{+/+}$ MEFs were infected with LGV-L2 for 30 hr, and F-actin was detected with Rhodamine-phalloidin. Note diffuse actin ring surrounding IncA positive inclusion in Vim$^{-/-}$ MEFs.

(D–F) Vimentin recruitment to the inclusion requires Rho-dependent F-actin assembly. HeLa cells infected with LGV-L2 for 30 hr were treated with Noc, CytoD, or C3 as in Figure 2; then, they were fixed and immunostained for vimentin and IncA. The percentage of vimentin-positive inclusions was determined in the presence of inhibitors (D) or after removal of Lat-B for 0–3 hr (F) (n = 150). Note reassembly of cages of vimentin (red) filaments around inclusions (arrows) after removal of Lat B (E). Host and bacterial DNA were detected with TO-PRO-3 (blue).

A Chlamydial Protease Cleaves Intermediate Filaments and Alters Their Cytoskeletal Properties

Although our results indicated that F-actin and IFs impart unusual structural stability to the inclusion, the formation of a rigid cage is incompatible with the organelles' need to expand to accommodate replicating bacteria. We observed that vimentin, keratin-8, and keratin-18 were processed to lower molecular weight forms in infected cells (Figure 5A). These findings suggested that cytoplasmic IF proteins may be selectively processed during infection. The *C. trachomatis* genome encodes two proteases that access the host cytoplasm to degrade transcription factors and signaling molecules important in immune responses (Lad et al., 2007; Zhong et al., 2001). One of these proteases, Chlamydial proteasome-like activity factor (CPAF), also targets cytokeratin-8 (Dong et al., 2004). To test if CPAF cleaves vimentin, we treated HeLa cell lysates with immunoprecipitated CPAF. This treatment resulted in the rapid cleavage of vimentin, cytokeratin-8, and cytokeratin-18 into fragments of similar in size to those seen during infection (Figure 5B). However, several additional cleavage products were observed in vivo. To test if the cleavage of IF proteins in vivo was mediated by CPAF, we treated infected cells with lactacystin, a proteosomal inhibitor that prevents CPAF activity at high concentrations (Zhong et al., 2001). Cleavage of IFs was blocked by lactacystin but not ALLN (N-acetyl-L-leucyl-L-leucyl-L-Norleucinal), an unrelated proteosomal inhibitor, suggesting that cleavage of IFs during infection was mediated by CPAF (Figure 5C). We isolated the terminal vimentin cleavage products and mapped the proteolytic cleavage site to Ser-72 in the amino-terminal Head domain (Figure 5D). Because the site of CPAF cleavage in vimentin is similar to that reported for cytokeratin-8 (Dong et al., 2004), we hypothesized that CPAF was able to target divergent IFs by recognizing the structurally conserved Rod and Tail domains. However, the Head domain of vimentin (aa 1–84) alone was an efficient substrate for CPAF cleavage in vitro (Figure 5E) and in vivo (not shown), indicating that despite the considerable primary amino acid sequence divergence of Head domains, conserved structural features in this domain are sufficient for CPAF recognition. Unfortunately, it has been difficult to map the CPAF recognition site or to generate CPAF-resistant versions of vimentin since mutations at the cleavage site unmask alternative cleavage sites in the serine-rich Head domain (not shown).

Because the Head domain of IF proteins is required for filament formation (Strelkov et al., 2003), we predicted that the cytoskeletal properties of Headless IFs would be different from those of intact proteins. We first tested the ability of IF proteins to cosediment with cytoskeletal structures. Unlike full-length IF proteins, which pelleted in the detergent-insoluble fraction, the processed vimentin and cytokeratin-8 were found in the soluble fraction (Figure 5F), indicating that the ability of these proteins to assemble into large, readily sedimentable structures is compromised in infected cells. When IF cleavage was inhibited with lactacystin, uncleaved IF proteins remained in the pellet indicating that CPAF-mediated cleavage of IFs was required for their detergent solubility (Figure 5G).

Despite their altered sedimentation properties, microscopical analysis of intact cells indicated that these modified IF proteins formed filamentous structures at the periphery of the inclusion (Figures 1A, 1B, and S2). Consistent with this, cleaved IFs formed high molecular weight (>200 kDa) complexes in the presence of low levels of chemical crosslinker that were indistinguishable from those formed in uninfected cells (Figure 5H and data not shown). In addition, cleaved keratin-8 and keratin-18 coimmunoprecipitated as heterotypic complexes in vivo and in vitro (Figure 5I and data not shown), indicating that CPAF processing did not lead to the disassembly of the basic IF subunit. To assess the fate of the Head domain in infected cells, we monitored the localization of an NH_2-terminal-tagged GFP-vimentin fusion protein. GFP-vimentin localized to filaments and to mature inclusions, even at stages where CPAF had cleaved the majority of the Head domain (Figures 6A and 6B). Based on these observations, we postulate that the CPAF-cleaved filaments did not

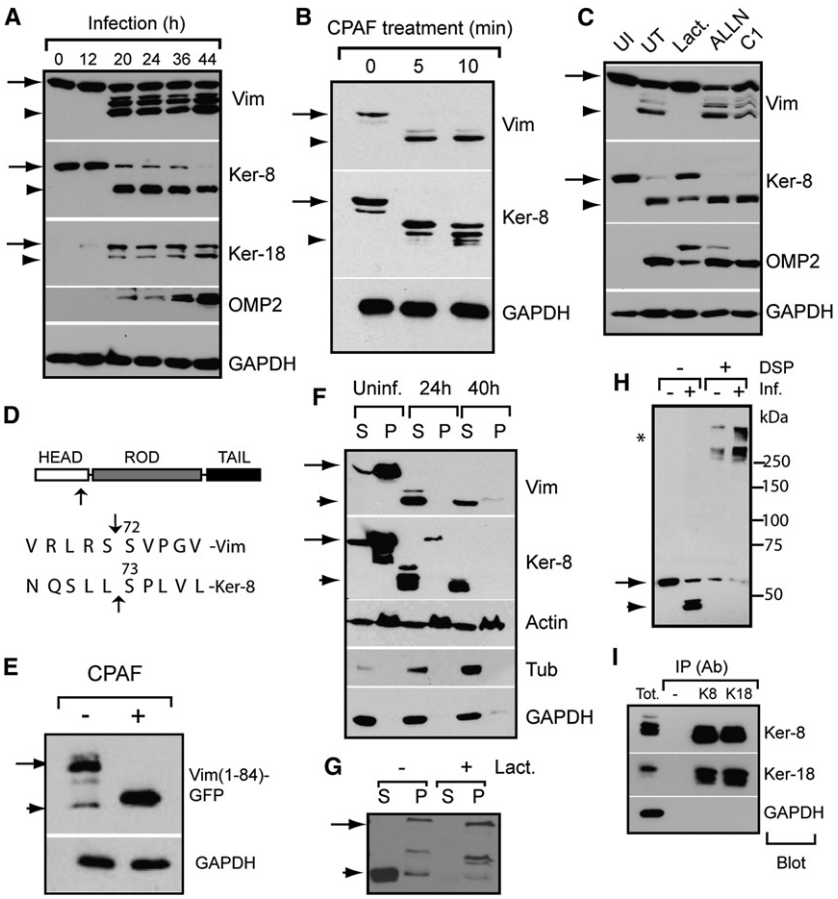

Figure 5. Proteolytic Processing of IF Proteins by CPAF Alters Its Cytoskeletal Properties

(A–D) The Head domain of IFs is cleaved by CPAF during infection. HeLa cells were infected with LGV-L2 for the indicated times. Total cell lysates were prepared, and proteins were identified by SDS-PAGE followed by immunoblots with specific antibodies. Note processing of vimentin, cytokeratin-8, and cytokeratin-18 (A). CPAF cleaved IFs in vitro (see Experimental Procedures) to generate fragments similar to those observed in vivo (B). Cleavage was inhibited in vivo by pretreatment with lactacystin but not by proteasome (ALLN) or Type III secretion inhibitors (C1) (C). The CPAF-cleavage site was determined by amino-terminal sequencing vimentin purified from infected cells and shown to map to Ser72 in the Head domain of the IF protein (D). For comparison, the CPAF-cleavage site for keratin-8 is shown (Dong et al., 2004).

(E) The Rod and Tail domains are not required for CPAF recognition of vimentin. Cell lysates from HeLa cells expressing the Head domain of vimentin (aa 1–84) fused to GFP were treated with CPAF for 30 min and analyzed by immunoblots.

(F and G) The cytoskeletal properties of IFs are altered by CPAF. HeLa cells were infected with LGV-L2 for 0 hr, 24 hr, or 40 hr, extracted with 1% Tx X-100, and subjected to differential centrifugation. Proteins in the detergent soluble and insoluble fractions were identified by immunobloting with specific antibodies. Note partitioning of the IF cleavage products (arrowheads) with the detergent soluble fractions. Lactacystin treatment prevented the partitioning of IFs to soluble fractions in infected cells (G).

(H) Cleaved vimentin is incorporated into high molecular weight complexes. Infected and uninfected HeLa cells were treated with the crosslinker DSP and the vimentin crosslinked complexes (*) were identified in nonreduced samples by immunoblotting.

(I) The formation of keratins 8/18 heterodimers is resistant to CPAF-mediated cleavage. Keratin-8 and keratin-18 were immunoprecipitated from infected HeLa lysates, and the coimmunoprecipitate of their cognate filament partners was assessed by immunoblots. Arrows indicate full-length IF protein, and arrowheads indicate processed forms of IF proteins.

disassemble because the "nicked" Head domain from pre-existing filaments remained associated with basic filament subunits via noncovalent interactions.

Overall, these results indicated that although IFs maintain their filamentous morphology, these structures may lose their structural scaffolding properties as they become progressively processed by CPAF. To test this, we assessed the subcellular localization of detergent-resistant vimentin at various time points postinfection. We observed an incremental loss of IFs from the vicinity of the inclusion after treatment of live cells with Tx-100 (Figure 6C). By 44 hr, all vimentin associated with inclusion was extracted while peripheral fibers remained intact (Figure 6C). We conclude that *Chlamydia* specifically alters the cytoskeletal properties of IFs filaments adjacent to the inclusion.

DISCUSSION

Chlamydiae are unique among intracellular bacterial pathogens in that maintenance of a large, stable membrane-bound parasitophorous vacuole may be central to the generation of developmental forms and ultimately determine the yield of infectious units (Peters et al., 2007). Here we present evidence that *Chlamydia* maintains the stability of such an organelle by co-opting the function of F-actin and intermediate filaments, a scaffolding cytoskeletal structure (Herrmann et al., 2007).

Many intracellular pathogens manipulate cytoskeletal functions at the plasma membrane to facilitate entry into host cells. For example, a range of Type III-secreted bacterial effectors mediate local bursts of actin polymerization at attachments sites by recruiting and activating nucleators of actin polymerization or by providing their own actin nucleation and bundling functions (Rottner et al., 2005). In turn, relatively less is known about the modulation of actin dynamics by membrane-bound intracellular bacteria. Pathogenic mycobacteria inhibit F-actin assembly at the surface of the bacteria-containing vacuole to inhibit fusion with lysosomes (Anes et al., 2003; Guerin and de Chastellier, 2000). In contrast, *Salmonella typhimurium*, recruits F-actin to the *Salmonella*-containing vacuole (SCV) (Meresse et al., 2001). The secreted effector SteC is required for F-actin assembly at the SCV, but it is unclear what actin modulators participate in this process or the role that F-actin assembly plays in SCV maintenance (Poh et al., 2008; Unsworth et al., 2004).

Our studies indicate that *C. trachomatis* co-opts RhoA function to assemble an F-actin ring at the surface of the inclusion

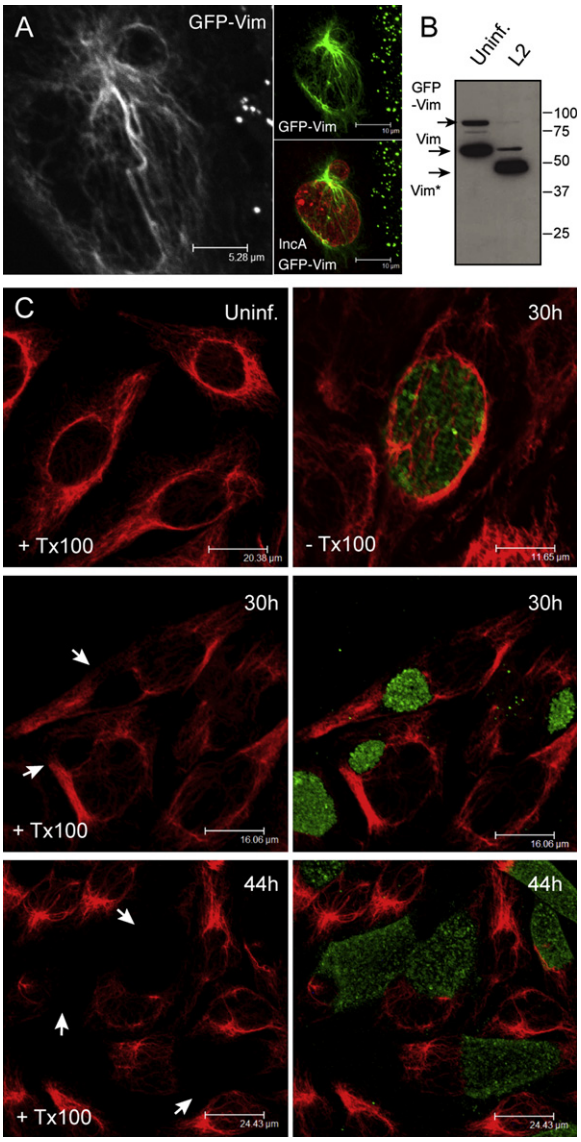

Figure 6. Vimentin Filaments at the Periphery of the Inclusion Are Sensitive to Detergent Extraction

(A-B) The cleaved Head domain of vimentin remains associated with inclusion filaments. HeLa cells expressing vimentin with an amino terminal GFP fusion (GFP-Vim) were infected with LGV-L2 for 24 hr and analyzed by fluorescence microscopy (A). Note GFP-vimentin in inclusion-associated filaments (A) despite complete cleavage of the tagged protein (B).

(C) Vimentin filaments at the periphery of the inclusion are preferentially sensitive to detergent extraction. HeLa cells were infected with LGV-L2 for 30–44 hr, solubilized with Tx-100, and immunostained with anti-vimentin (red) and anti-chlamydial (green) antibodies. Note progressive detergent sensitivity of vimentin filaments associated with the inclusion periphery. As a reference, note compact IF cage present in nondetergent-treated infected cells (upper right panel) is shown.

(Figure 3). The role of RhoA in the assembly of F-actin rings at the inclusion is likely to be direct since the GTPases Rac1 and Cdc42, regulators of actin dynamics whose activity can indirectly influence RhoA (Burridge and Wennerberg, 2004), were not required for the formation of actin rings (Figure 3C). Furthermore, exogenously expressed RhoA was recruited to the periphery of the inclusion independently of its nucleotide-bound state (Figures 3D and 3E), suggesting that F-actin assembly at the inclusion maybe initiated directly by RhoA. However, although F-actin at the inclusion resembled stress fibers, its assembly was independent of canonical RhoA targets (Figure 3A), indicating a novel mechanism for maintenance of these RhoA-dependent structures. By analogy to other bacterial pathogens, we hypothesize that secreted chlamydial proteins recruit RhoA to the surface of the inclusion.

In addition to F-actin rings, a cage of IFs is assembled on the mature *Chlamydia* inclusion. A remodeling of IF networks has been reported during viral (Stefanovic et al., 2005) and protozoan (Halonen and Weidner, 1994) infections. Similarly, for bacterial pathogens, IFs are recruited to plasma membrane ruffles formed during *Salmonella* invasion (Carlson et al., 2002) and at enteropathogenic *E. coli* attachment sites (Batchelor et al., 2004). However, the functional role of IF remodeling by these pathogens is unclear.

Because of their high tensile strength, IFs have been implicated in providing mechanical support to cells and tissues (Kim and Coulombe, 2007). This function is consistent with our observation that the inclusion is enveloped in a stable cytoskeletal scaffold (Figure 1) and that vimentin is necessary for the structural stability to the inclusion (Figures 4A and 4B). Unexpectedly, we found that the chlamydial protease CPAF cleaved the Head domain of vimentin, which is essential for filament assembly in vitro (Herrmann et al., 1996) and that cleavage took place at an analogous site to what has been reported for cytokeratin-8 (Dong et al., 2004) (Figure 5). It has been proposed that disruption of cytokeratin-8 would allow expansion of the inclusion by removing the physical constraints imposed by these static cytoskeletal structures on inclusion expansion (Dong et al., 2004). Our findings indicated that CPAF-cleaved vimentin, cytokeratin-8, and keratin-18 remained morphologically (Figure 1) as filamentous forms and retained many of their polymer functions (Figures 5H and 5I). We postulate that formation of IF filaments was not compromised after CPAF-mediated cleavage because the Head domain remained associated with filaments (Figure 6A) and because F-actin at the inclusion helped stabilize filaments by direct binding or by plakin-like bridging proteins (Fuchs and Karakesisoglou, 2001). Indeed, inhibition of F-actin assembly at the inclusion with Lat-B or C3-transferase led to the loss of vimentin filaments from the inclusion (Figures 4D–4F). Nonetheless, CPAF-modified IFs were sensitive to detergent extraction (Figures 5F and 5G), suggesting that these polymers lack the structural properties of uncleaved vimentin and cytokeratin filaments. Consistent with this, filaments proximal to the inclusion became progressively sensitive to detergent extraction (Figure 6C).

Overall, these results lead us to propose a model wherein RhoA-mediated F-actin assembly at the surface of the inclusion is followed by the recruitment of IF proteins. These IFs are progressively nicked by CPAF to form a "bilayered" cage of F-actin and modified IFs (Figure 7). This cage provides structural support to the inclusion yet becomes increasingly flexible to accommodate exponential bacterial replication and inclusion expansion. Given our observation that transient disruption of inclusion integrity leads to the leakage of inclusion contents and a robust activation of IL-8 expression (Figure 2), we hypothesize that one reason why *Chlamydia* assembles stable cytoskeletal scaffolds on the inclusion is to limit the exposure of bacterial

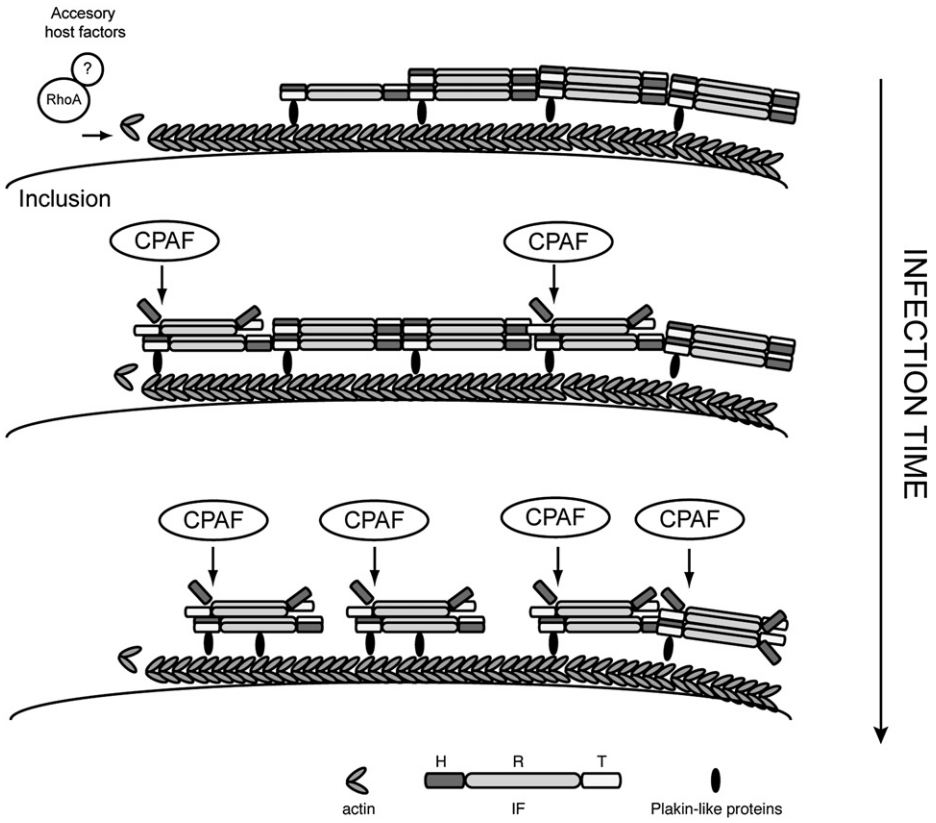

Figure 7. A Model for Actin and Intermediate Filament Assembly at the Surface of the *Chlamydia* Inclusion

C. trachomatis effectors at the inclusion membrane recruit RhoA to trigger F-actin assembly. F-actin at the inclusion helps recruit and stabilize IFs possibly via linker molecules to form a stable support cage for the inclusion. As the inclusion expands, the secreted chlamydial protease-CPAF progressively cleaves the Head domain of preassembled filaments to increase their flexibility while retaining some of their structural functions.

products to cytoplasmic innate immune surveillance pathways (Buchholz and Stephens, 2008). In addition, CPAF-mediated disruption of IFs during infection may result in defects in cell migration, wound repair (Eckes et al., 2000), and infiltration by immune effector cells (Nieminen et al., 2006). Since the reorganization and cleavage of IFs is conserved among all *Chlamydia* and *Chlamydophila* species we have tested (Figure S3), we speculate that F-actin and IF remodeling are central in chlamydial pathogenesis. The full consequence of disrupting the IF network of infected cells on the pathogenesis of chlamydial disease may not become apparent until the development of appropriate tissue and animal infection models for *C. trachomatis*.

Our findings detail a unique mechanism of cytoskeletal subversion by an intracellular pathogen. Furthermore, it highlights the importance of proteases like CPAF as central, evolutionarily conserved virulence factors that can co-opt a range of host cellular functions. These virulence factors are prime candidates for the screening and development of small molecule inhibitors with potential anti-chlamydial activity.

EXPERIMENTAL PROCEDURES

Reagents

The inhibitors used were nocodazole and cytochalasin D (Sigma), LatA and LatB (Invitrogen), blebbistatin, and lactacystin (EMD Biosciences), C3 transferase (Cytoskeleton, Inc.), C1 (ChemBridge), and ALLN (Biomol).

Cell Culture and Bacterial Infections

HeLa cells (ATCC), MFT-16 (Vim$^{-/-}$), and MFT-6 (Vim$^{+/+}$) MEFs (R. Evans, UCHS, CO) were grown in DMEM/F12 (1:1 mix; Invitrogen) and supplemented with 10% fetal bovine serum (FBS) (CellGro Mediatech, Inc.). *C. trachomatis* serovar LGV-L2 was obtained from R. Stephens (UC Berkeley). Elementary bodies (EBs) were purified by density gradients and stored in SPG (0.25 M sucrose, 10 mM sodium phosphate, 5 mM L-glutamic acid) buffer at −80°C. Infection of HeLa and MEFs was synchronized by centrifugation (3000 × *g* for 30 min at 10°C) of EBs onto cell monolayers.

Plasmid Constructs, siRNA Transfections, and RT-PCR

Plasmids expressing NH_2-terminal GFP-tagged full-length vimentin (Ho et al., 1998) and Head domains (aa 1–84) (Byun et al., 2001) were from R.K. Liem (Columbia University, NY) and V. Cryns (Northwestern University, Chicago), respectively. Plasmids expressing RhoA, RhoA T19N (dominant negative), and RhoA Q63L (constitutively active) were obtained from S. Abraham (Duke University, NC). Plasmids were transfected into HeLa cells with Fugene (Roche Applied Sciences), as detailed by the manufacturer. For siRNA transfections, 2 × 10^4 HeLa cells were plated in 24 well plates and transfected with 0.5 μg of siRNA oligonucleotide mixes specific for Rac-1, CDC42, RhoA, or scrambled sequence (QIAGEN) using RNAi-fect transfection reagent (QIAGEN). After 24 hr, transfected cells were infected with LGV-L2, retransfected with 0.5 μg of siRNA for an additional 24 hr, fixed, and processed for immunofluorescence. The efficiency of siRNA knockdowns and the analysis of IL-8 transcript levels were assessed as detailed in Figure S5.

Microscopy

A detailed list of antibodies is available in the Supplemental Data. F-actin was detected with rhodamine-conjugated phalloidin (15 U/ml, Invitrogen). Bacterial

and host DNA were detected with To-Pro-3 (Invitrogen). For indirect immunofluorescence, HeLa cells were grown on glass coverslips, fixed with 3% paraformaldehyde (PFA) in phosphate-buffered saline (PBS) for 10 min, and postfixed with ice-cold methanol. After blocking with 2% bovine serum albumin (BSA)-PBS, cells were treated with specific antibodies against IF proteins followed by Alexa-conjugated secondary antibodies (Invitrogen). For phalloidin stains, fixation was performed with 3% PFA followed by permeabilization with 0.2% Triton X-100 in PBS. Fluorescent images were acquired using a Leica TCS Laser Confocal Scanning Microscope and processed with Leica software. Live-cell methods are available in the Supplemental Data.

For transmission electron microscopy (TEM), HeLa cells were grown on plastic thermanox coverslips and infected with LGV-L2 for 30 hr. Live cells were treated with 1% Triton X-100 for 5 min on ice and fixed with 2% glutaraldehyde/2% tannic acid/0.025% saponin, postfixed with 0.4% osmium tetroxide, and followed by 1% uranyl acetate. This procedure stabilizes cytoskeletal filaments (Maupin and Pollard, 1983). Cells were then dehydrated by graded ethanol extraction and embedded in Spurr's resin. Thin sections were prepared and poststained with lead citrate before imaging on a Tecnai 12 Transmission Electron Microscope (FEI Company).

CPAF-Cleavage Assays

Crude cell lysates were prepared from a confluent 10 cm dish of infected HeLa cells by solubilization in TNEX (20 mM Tris-HCl [pH 8.0], 150 mM NaCl, 2 mM EDTA, and 1% Triton X-100) buffer supplemented with a broad protease inhibitor cocktail (Roche Diagnostics). Anti-CPAF mAb was immobilized on Protein-G Sepharose beads (Amersham) and incubated with infected cell lysates for 3 hr followed by extensive washing in TNEX. To perform in vitro cleavage assays, aliquots of HeLa lysates (prepared as described above) were incubated with CPAF-Sepharose beads on ice. Proteolysis was initiated by placing reactions at 37°C and 50 μl aliquots were removed, mixed with SDS sample buffer, and heated at 65°C for 10 min. To determine the site of CPAF proteolysis, vimentin was immunoprecipitated (IP) from the TNEX-lysed infected cells with anti-vimentin mAbs (V9) crosslinked to Protein-G-Sepharose beads. The bound vimentin was eluted from the beads in 0.2 M glycine (pH 2.5), precipitated with ice-cold acetone, and electrotransferred to PVDF membranes after SDS PAGE. The protein band was excised from the membranes, and the N-terminal sequence was determined by Edman degradation at Iowa State University Protein Facility (Iowa State University, IA).

Biochemical Analysis of Intermediate Filaments

Detergent Solubility Assays

To assess the cytoskeletal properties of IF proteins, we performed differential centrifugation assays after detergent solubilization. In brief, HeLa cells grown in 10 cm dishes were infected with LGV-L2 for 20 hr or 40 hr. The cells were lysed in TNEX buffer supplemented with a protease inhibitor cocktail, 50 μM lactacystin, and 10 U/mL DNase-1 (Invitrogen). Samples were centrifuged at 20,000 × g for 10 min. The insoluble pellet was washed twice with TNEX and solubilized in SDS sample buffer.

Chemical Crosslinking Methods

HeLa cells grown were infected with LGV-L2 for 30 hr, washed with Hank's balanced salt solution (HBSS), and treated with 1 mM dithiobis-(succinimidyl propionate) (DSP) (Pierce) in HBSS on ice for 20 min. The cells were washed with HBSS and quenched with 50 mM glycine in HBSS for 15 min on ice. PNS from TNEX-lysed cells were mixed with SDS sample buffer without reducing agent and heated for 10 min at 65°C. For the keratin-8 and keratin-18 coimmunoprecipitation (coIP), HeLa cells were infected with LGV-L2 for 30 hr and lysed in TNEX. Cytokeratins were immunoprecipitated with anti-keratin-8 or anti-keratin-18 monoclonal antibodies coupled to Protein-G Sepharose beads (Amersham). Immunoprecipitated proteins were solubilized in Laemmli sample buffer, followed by SDS-PAGE and immunoblot analysis. All protein samples were analyzed by SDS-PAGE and immunoblotting with specific antibodies.

SUPPLEMENTAL DATA

Supplemental Data include five figures, Supplemental Experimental Procedures, and can be found online at http://www.cellhostandmicrobe.com/cgi/content/full/4/2/159/DC1/.

ACKNOWLEDGMENTS

We thank S. Abraham, H. Caldwell, T. Hackstadt, R. Evans, V. Cryns, R.K. Liem, and G. Zhong, for their kind gifts of cell lines, expression plasmids, and antibodies; and J. Cocchiaro, D. Lew, and J. Heitman for comments on the manuscript. This work was supported by funds from the Whitehead Foundation, the Pew Scholars Program, the NIH (AI068032), and the Burroughs Wellcome Trust Fund.

Received: January 21, 2008
Revised: April 29, 2008
Accepted: May 23, 2008
Published: August 13, 2008

REFERENCES

Aktories, K., and Just, I. (2005). Clostridial Rho-inhibiting protein toxins. Curr. Top. Microbiol. Immunol. *291*, 113–145.

Anes, E., Kuhnel, M.P., Bos, E., Moniz-Pereira, J., Habermann, A., and Griffiths, G. (2003). Selected lipids activate phagosome actin assembly and maturation resulting in killing of pathogenic mycobacteria. Nat. Cell Biol. *5*, 793–802.

Batchelor, M., Guignot, J., Patel, A., Cummings, N., Cleary, J., Knutton, S., Holden, D.W., Connerton, I., and Frankel, G. (2004). Involvement of the intermediate filament protein cytokeratin-18 in actin pedestal formation during EPEC infection. EMBO Rep. *5*, 104–110.

Beatty, W.L. (2006). Trafficking from CD63-positive late endocytic multivesicular bodies is essential for intracellular development of Chlamydia trachomatis. J. Cell Sci. *119*, 350–359.

Belland, R., Ojcius, D.M., and Byrne, G.I. (2004). Chlamydia. Nat. Rev. Microbiol. *2*, 530–531.

Brown, W.J., Skeiky, Y.A., Probst, P., and Rockey, D.D. (2002). Chlamydial antigens colocalize within IncA-laden fibers extending from the inclusion membrane into the host cytosol. Infect. Immun. *70*, 5860–5864.

Buchholz, K.R., and Stephens, R.S. (2007). The extracellular signal-regulated kinase/mitogen-activated protein kinase pathway induces the inflammatory factor interleukin-8 following Chlamydia trachomatis infection. Infect. Immun. *75*, 5924–5929.

Buchholz, K.R., and Stephens, R.S. (2008). The cytosolic pattern recognition receptor NOD1 induces inflammatory IL-8 during Chlamydia trachomatis infection. Infect. Immun. *76*, 3150–3155.

Burridge, K., and Wennerberg, K. (2004). Rho and Rac take center stage. Cell *116*, 167–179.

Byun, Y., Chen, F., Chang, R., Trivedi, M., Green, K.J., and Cryns, V.L. (2001). Caspase cleavage of vimentin disrupts intermediate filaments and promotes apoptosis. Cell Death Differ. *8*, 443–450.

Carabeo, R.A., Grieshaber, S.S., Fischer, E., and Hackstadt, T. (2002). Chlamydia trachomatis induces remodeling of the actin cytoskeleton during attachment and entry into HeLa cells. Infect. Immun. *70*, 3793–3803.

Carabeo, R.A., Mead, D.J., and Hackstadt, T. (2003). Golgi-dependent transport of cholesterol to the Chlamydia trachomatis inclusion. Proc. Natl. Acad. Sci. USA *100*, 6771–6776.

Carlson, S.A., Omary, M.B., and Jones, B.D. (2002). Identification of cytokeratins as accessory mediators of Salmonella entry into eukaryotic cells. Life Sci. *70*, 1415–1426.

Clifton, D.R., Fields, K.A., Grieshaber, S.S., Dooley, C.A., Fischer, E.R., Mead, D.J., Carabeo, R.A., and Hackstadt, T. (2004). A chlamydial type III translocated protein is tyrosine-phosphorylated at the site of entry and associated with recruitment of actin. Proc. Natl. Acad. Sci. USA *101*, 10166–10171.

Cocchiaro, J., Kumar, Y., Fischer, E., Hackstadt, T., and Valdivia, R.H. (2008). Cytoplasmic lipid droplets are translocated into the lumen of the Chlamydia trachomatis parasitophorous vacuole. Proc. Natl. Acad. Sci. USA *105*, 9379–9384.

Colucci-Guyon, E., Portier, M.M., Dunia, I., Paulin, D., Pournin, S., and Babinet, C. (1994). Mice lacking vimentin develop and reproduce without an obvious phenotype. Cell *79*, 679–694.

Desai, A., and Mitchison, T.J. (1997). Microtubule polymerization dynamics. Annu. Rev. Cell Dev. Biol. *13*, 83–117.

Dong, F., Su, H., Huang, Y., Zhong, Y., and Zhong, G. (2004). Cleavage of host keratin 8 by a Chlamydia-secreted protease. Infect. Immun. *72*, 3863–3868.

Eckes, B., Colucci-Guyon, E., Smola, H., Nodder, S., Babinet, C., Krieg, T., and Martin, P. (2000). Impaired wound healing in embryonic and adult mice lacking vimentin. J. Cell Sci. *113*, 2455–2462.

Fenteany, G., and Zhu, S. (2003). Small-molecule inhibitors of actin dynamics and cell motility. Curr. Top. Med. Chem. *3*, 593–616.

Fuchs, E., and Karakesisoglou, I. (2001). Bridging cytoskeletal intersections. Genes Dev. *15*, 1–14.

Grieshaber, S.S., Grieshaber, N.A., and Hackstadt, T. (2003). Chlamydia trachomatis uses host cell dynein to traffic to the microtubule-organizing center in a p50 dynamitin-independent process. J. Cell Sci. *116*, 3793–3802.

Guerin, I., and de Chastellier, C. (2000). Disruption of the actin filament network affects delivery of endocytic contents marker to phagosomes with early endosome characteristics: the case of phagosomes with pathogenic mycobacteria. Eur. J. Cell Biol. *79*, 735–749.

Halonen, S.K., and Weidner, E. (1994). Overcoating of Toxoplasma parasitophorous vacuoles with host cell vimentin type intermediate filaments. J. Eukaryot. Microbiol. *41*, 65–71.

Herrmann, H., Haner, M., Brettel, M., Muller, S.A., Goldie, K.N., Fedtke, B., Lustig, A., Franke, W.W., and Aebi, U. (1996). Structure and assembly properties of the intermediate filament protein vimentin: the role of its head, rod and tail domains. J. Mol. Biol. *264*, 933–953.

Herrmann, H., Bar, H., Kreplak, L., Strelkov, S.V., and Aebi, U. (2007). Intermediate filaments: from cell architecture to nanomechanics. Nat. Rev. Mol. Cell Biol. *8*, 562–573.

Ho, C.L., Martys, J.L., Mikhailov, A., Gundersen, G.G., and Liem, R.K. (1998). Novel features of intermediate filament dynamics revealed by green fluorescent protein chimeras. J. Cell Sci. *111*, 1767–1778.

Hotulainen, P., and Lappalainen, P. (2006). Stress fibers are generated by two distinct actin assembly mechanisms in motile cells. J. Cell Biol. *173*, 383–394.

Hybiske, K., and Stephens, R.S. (2007). Mechanisms of host cell exit by the intracellular bacterium Chlamydia. Proc. Natl. Acad. Sci. USA *104*, 11430–11435.

Jaffe, A.B., and Hall, A. (2005). Rho GTPases: biochemistry and biology. Annu. Rev. Cell Dev. Biol. *21*, 247–269.

Katoh, K., Kano, Y., and Ookawara, S. (2007). Rho-kinase dependent organization of stress fibers and focal adhesions in cultured fibroblasts. Genes Cells *12*, 623–638.

Kim, S., and Coulombe, P.A. (2007). Intermediate filament scaffolds fulfill mechanical, organizational, and signaling functions in the cytoplasm. Genes Dev. *21*, 1581–1597.

Lad, S.P., Yang, G., Scott, D.A., Wang, G., Nair, P., Mathison, J., Reddy, V.S., and Li, E. (2007). Chlamydial CT441 is a PDZ domain-containing tail-specific protease that interferes with the NF-kappaB pathway of immune response. J. Bacteriol. *189*, 6619–6625.

Maupin, P., and Pollard, T.D. (1983). Improved preservation and staining of HeLa cell actin filaments, clathrin-coated membranes, and other cytoplasmic structures by tannic acid-glutaraldehyde-saponin fixation. J. Cell Biol. *96*, 51–62.

Meresse, S., Unsworth, K.E., Habermann, A., Griffiths, G., Fang, F., Martinez-Lorenzo, M.J., Waterman, S.R., Gorvel, J.P., and Holden, D.W. (2001). Remodelling of the actin cytoskeleton is essential for replication of intravacuolar Salmonella. Cell. Microbiol. *3*, 567–577.

Musch, A. (2004). Microtubule organization and function in epithelial cells. Traffic *5*, 1–9.

Narumiya, S., Ishizaki, T., and Uehata, M. (2000). Use and properties of ROCK-specific inhibitor Y-27632. Methods Enzymol. *325*, 273–284.

Nieminen, M., Henttinen, T., Merinen, M., Marttila-Ichihara, F., Eriksson, J.E., and Jalkanen, S. (2006). Vimentin function in lymphocyte adhesion and transcellular migration. Nat. Cell Biol. *8*, 156–162.

Peters, J., Wilson, D.P., Myers, G., Timms, P., and Bavoil, P.M. (2007). Type III secretion a la Chlamydia. Trends Microbiol. *15*, 241–251.

Poh, J., Odendall, C., Spanos, A., Boyle, C., Liu, M., Freemont, P., and Holden, D.W. (2008). SteC is a Salmonella kinase required for SPI-2-dependent F-actin remodelling. Cell. Microbiol. *10*, 20–30.

Rodriguez-Boulan, E., Kreitzer, G., and Musch, A. (2005). Organization of vesicular trafficking in epithelia. Nat. Rev. Mol. Cell Biol. *6*, 233–247.

Rottner, K., Stradal, T.E., and Wehland, J. (2005). Bacteria-host-cell interactions at the plasma membrane: stories on actin cytoskeleton subversion. Dev. Cell *9*, 3–17.

Schachter, J. (1999). Infection and disease epidemiology. In Chlamydia: Intracellular Biology, Pathogenesis and Immunity, R.S. Stephens, ed. (Washington, DC: ASM), pp. 31.

Stefanovic, S., Windsor, M., Nagata, K.I., Inagaki, M., and Wileman, T. (2005). Vimentin rearrangement during African swine fever virus infection involves retrograde transport along microtubules and phosphorylation of vimentin by calcium calmodulin kinase II. J. Virol. *79*, 11766–11775.

Straight, A.F., Cheung, A., Limouze, J., Chen, I., Westwood, N.J., Sellers, J.R., and Mitchison, T.J. (2003). Dissecting temporal and spatial control of cytokinesis with a myosin II Inhibitor. Science *299*, 1743–1747.

Strelkov, S.V., Herrmann, H., and Aebi, U. (2003). Molecular architecture of intermediate filaments. Bioessays *25*, 243–251.

Toivola, D.M., Tao, G.Z., Habtezion, A., Liao, J., and Omary, M.B. (2005). Cellular integrity plus: organelle-related and protein-targeting functions of intermediate filaments. Trends Cell Biol. *15*, 608–617.

Unsworth, K.E., Way, M., McNiven, M., Machesky, L., and Holden, D.W. (2004). Analysis of the mechanisms of Salmonella-induced actin assembly during invasion of host cells and intracellular replication. Cell. Microbiol. *6*, 1041–1055.

Vale, R.D., Ignatius, M.J., and Shooter, E.M. (1985). Association of nerve growth factor receptors with the triton X-100 cytoskeleton of PC12 cells. J. Neurosci. *5*, 2762–2770.

Wear, M.A., Schafer, D.A., and Cooper, J.A. (2000). Actin dynamics: assembly and disassembly of actin networks. Curr. Biol. *10*, R891–R895.

Wheeler, A.P., and Ridley, A.J. (2004). Why three Rho proteins? RhoA, RhoB, RhoC, and cell motility. Exp. Cell Res. *301*, 43–49.

Wilson, D.P., Timms, P., McElwain, D.L., and Bavoil, P.M. (2006). Type III secretion, contact-dependent model for the intracellular development of chlamydia. Bull. Math. Biol. *68*, 161–178.

Zhong, G., Fan, P., Ji, H., Dong, F., and Huang, Y. (2001). Identification of a chlamydial protease-like activity factor responsible for the degradation of host transcription factors. J. Exp. Med. *193*, 935–942.